28 Clinical Magnetic Resonance Neuroimaging in Mild Cognitive Impairment and Alzheimer Disease

Nicolás Fayed, Javier Garcia-Campayo, and Laura Viguera

Introduction

Amnestic mild cognitive impairment (MCI) is a common condition in the elderly individuals mainly characterized by memory loss. Although there may be other subtle decline in other functions, the general cognitive function and daily living activities are preserved [1].

The annual rate of conversion to dementia is around 12 %, in general to Alzheimer type dementia. In this review, we are focusing on the application of biochemical markers [2] and imaging techniques such as computed tomography (CT), magnetic resonance imaging (MRI), and positron emission tomography (PET). MRI can cover structural MRI that uses parametric quantitative methods such as volumetry, but also other techniques such as functional MRI (fMRI), diffusion/diffusion tensor imaging (DTI), arterial spin labeling (ASL) perfusion, and magnetic resonance spectroscopy (MRS) techniques. In this review we focus on the applications of MRI techniques and their role in cases of cognitive decline.

The relationship between dementia and parameters evaluated by imaging probably vary with age: amyloid load may not be as specific for cognitive impairment in very old patients as compared with younger patients, whereas indices of neuronal loss (regional volumes, metabolic activity, or absolute blood flow) might show a more stable relationship to dementia across ages [3]. Brain reserve will also influence the results from those studies. In Alzheimer disease (AD), large areas of medial temporal cortex are activated during cognitive tasks that do not occur in controls. This may represent a compensation for the reduction of function or a "cognitive reserve". Recommendations on the use of imaging techniques must be interpreted in light of such factors, whatever the technique used.

For the initial assessment of patients presenting with cognitive difficulties/symptoms of dementia, guidelines from several countries indicate that structural neuroimaging with CT or MRI is appropriate.

Space-occupying lesions, usually neoplasms or subdural hematomas, can be detected and may present progressive cognitive impairment. These lesions are uncommon, with estimations at approximately 3 % [4].

N. Fayed (✉)
Department of Neuroradiology, Quirón Hospital, Zaragoza, Spain
e-mail: nicola33fr@yahoo.es

J. Garcia-Campayo
Department of Psychiatry, Miguel Servet Hospital, University of Zaragoza, Zaragoza, Spain
e-mail: jgarcamp@gmail.com

L. Viguera
Preventative Activities and Health Promotion Network (REDIAPP), Zaragoza, Spain
e-mail: lauraviguera@gmail.com

P.Á. Gargiulo, H.L. Mesones Arroyo (eds.), *Psychiatry and Neuroscience Update*,
DOI 10.1007/978-3-319-17103-6_28

Magnetic Resonance Spectroscopy

MRS enables us to study the chemical composition of living tissues. It is based on the chemical shift of atoms. The concentration of some metabolites is determined from spectra that may be acquired in several ways.

Physical Basis of MRS

Currently the spectra may be acquired with single-voxel (SV) or multi-voxel (MV) techniques. The SV technique is readily available on most scanners. Voxels must be positioned away from sources of susceptibility artifacts and lipids. For diffuse processes, a 2 × 2 × 2-cm (8 cm^3) voxel is routinely used (See Fig. 28.1). A voxel (*volumetric pixel* or *Volumetric Picture Element*) is a volume element, representing a value on a regular grid in a three-dimensional (3D) space. In contrast to pixels and voxels, points and polygons are often explicitly represented by the coordinates of their vertices. A direct consequence of this difference is that polygons are able to efficiently represent simple 3D structures with a lot of empty or homogeneously filled space, while voxels are good at representing regularly sampled spaces that are non-homogeneously filled. Voxels are frequently used in the visualization and analysis of medical and scientific data. Some volumetric displays use voxels to describe their resolution. For example, a display might be able to show 512 × 512 × 512 voxels. For local lesions, the SV can be reduced in volume. The SV technique offers the advantages of better spatial location, more homogeneity, better water suppression, and speed. However, only one spectrum can be obtained per acquisition and the MV technique makes it possible to obtain multiple spectra simultaneously per acquisition and to assess a greater area of the brain but with smaller spectral resolution.

To date, the SV is still superior to MV on the grounds of reproducibility [5, 6]. For both SV and MV, the magnetic resonance scanner uses a process known as shimming to narrow peak line widths within the spectra. For SV studies, improving field homogeneity is performed with basic, zero-ordered shimming on clinical magnetic resonance scanners. For MV, the simultaneous production of uniform field homogeneity in multiple regions requires higher order shimming. To obtain high-quality spectra, blood products, air, fat, necrotic areas, cerebrospinal fluid, metal, calcification, and bone should be avoided. In such areas differing magnetic susceptibility results in a non-homogenous field that hinders the production of diagnostic quality spectra.

Two different approaches are generally used for proton spectroscopy of the brain: 1) SV methods based on the stimulated echo acquisition mode (STEAM) and 2) point resolved spectroscopy (PRESS) pulse sequences and spectroscopy imaging, also known as chemical shift imaging. These latter studies are usually done in two dimensions, using a variety of different pulse sequences (spin-echo, usually PRESS). The basic principle underlying SV localization techniques is to use three mutually orthogonal slice selective pulses and design the pulse sequence to collect only the echo signal from the point (voxel) in space where all three slices intersect. The PRESS mode is used more often than STEAM because it increases the signal/noise ratio and is less sensitive to movement artifacts [7].

Echo time (TE) have not yet standardized so far in MRS. In degenerative, demyelinating, and vascular disease a short TE is advocated. A short TE (20–40 ms) allows us to increase the signal/noise ratio and to visualize most metabolite peaks, with the inconvenience of some degree of overlapping of peaks. Intermediate TE (135–144 ms) inverts the lactate peak to better distinguish it from lipids peak. Long TE (270–288 ms) gives worse signal/noise ratio but allows better visualization of some peaks (N-cetylaspartate [NAA], choline [Chow], and creatine [Cr]). Time matters in clinical practice, so short TEs are preferable. In our experience with a 1.5 T General Electric Signa Horizon-clinical scanner a TE of 30 ms and a repetition time of 2500 ms has proven valuable [8].

A TE averaged PRESS technique has been yielding highly simplified spectra with better suppression of signals not pertaining to assessed

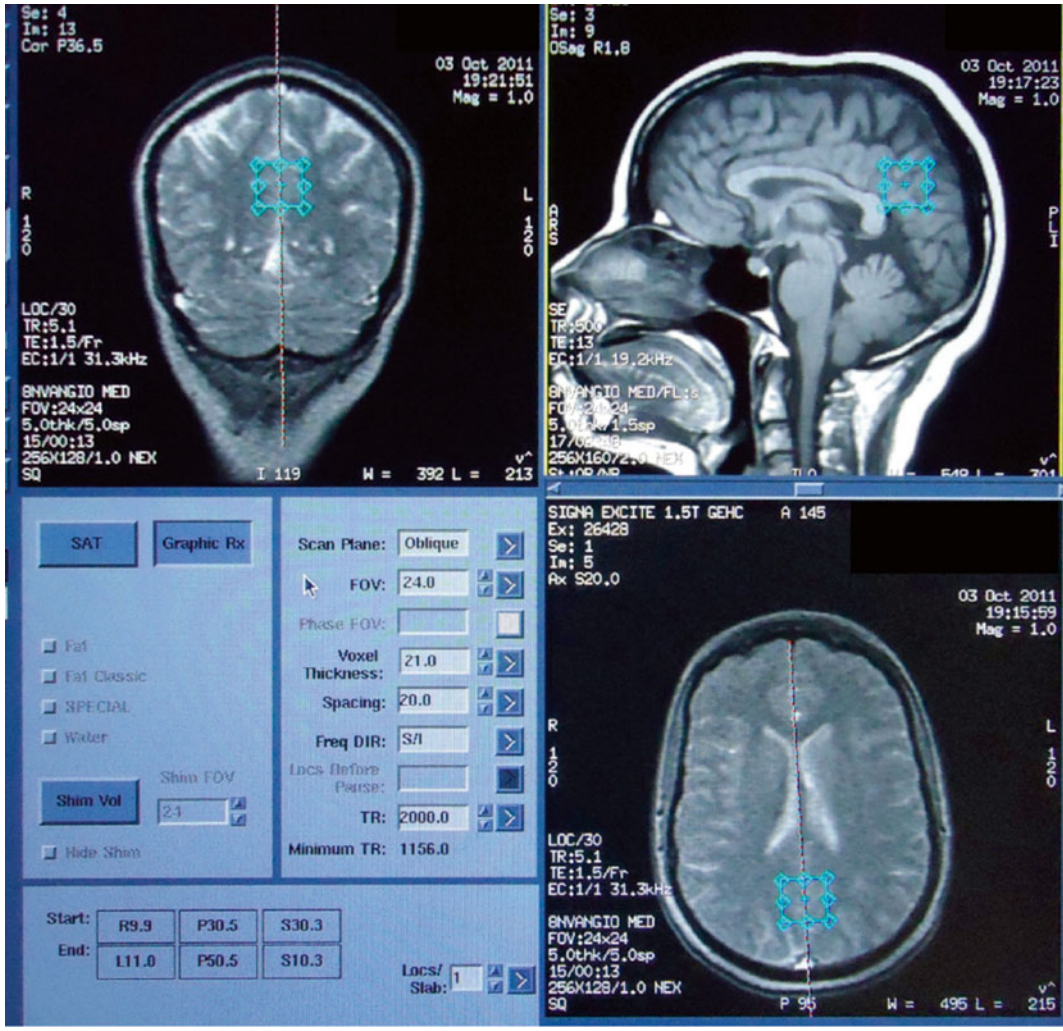

Fig. 28.1 Positioning of a single-voxel in the bilateral posteromedial parietal cortex for study with frontal, sagittal, and axial slices. The area explored includes the posterior cingulate gyrus

metabolites, such as that of macromolecules. TE is increased from 35 ms to 355 ms in steps of 2.5 ms with two acquisitions per step [9].

The most commonly used spectroscopy is that originating from a hydrogen nucleus (proton 1H-MRS). This technique is based on the differences in resonance obtained from hydrogen nuclei depending on the surrounding atoms (chemical shift). Each metabolite being assessed discloses a different hydrogen resonance frequency and appears in a different site in the spectrum. The position of the metabolite signal is identified on the horizontal axis by its chemical shift, scaled in units referred to as parts per million (ppm). With the appropriate factors considered, such as the number of protons, relaxation times and so forth, a signal can be converted into a metabolite concentration by measuring the area under the curve. Because water is the main component of living beings and its concentration is much higher than that of metabolites, it becomes necessary to suppress the resonance signal from the hydrogen of water. A plot showing peak amplitudes and frequencies is obtained.

Each spectrum shows peaks corresponding to the different metabolite values: myo-inositol

(mI), 3.56 and 4.06 ppm; Chow, 3.23 ppm; Cr, 3.03 and 3.94 ppm; NAA, 2.02; 2.5 and 2.6 ppm; glutamine and glutamate, 2.1–2.55 ppm and 3.8 ppm (See Fig. 28.2). Ratios between metabolites and Cr are also of great value as they counteract the systematic errors of measurements.

A program, called a linear combination (LC) model [10], fits in vivo spectra as a linear superposition of high-resolution "basis" spectra that are acquired from model solutions of the metabolites present in the region of interest. Advantages of an LC model are that all pre-processing steps, automatic phase correction, as well as modelling of a smooth baseline are included. Standardized basis sets are available for the most common clinical magnetic resonance machines (both 1.5 and 3 T).

Evolution of Brain Metabolites over the Lifetime

When analyzing metabolite levels in the whole sample while controlling for age and gender, we observe that all metabolites are correlated with age. NAA, glutamate and glutamate + glutamine and their ratios to Cr show a negative correlation (increase in age with a decrease in metabolite levels and vice versa), while the remaining metabolites, such as mI and Chow, show a direct correlation (See Fig. 28.3). A decrease in glutamate and glutamate + glutamine over one's lifetime, which is associated with a certain cognitive deterioration, could be expected as significant lower levels of these metabolites are found in AD. There is a certain degree of controversy in the literature regarding the changes in metabolite concentrations and ratios that occur with aging. Estimates of age effects based on such designs are interferred by secular changes in nutrition, medical care, and other factors.

MRS in Mild Cognitive Impairment and AD

Altered levels of NAA or NAA/Cr ratios are the most common finding reported in patients with AD and MCI [11–13], although alterations in other metabolites including mI [14] and glutamate

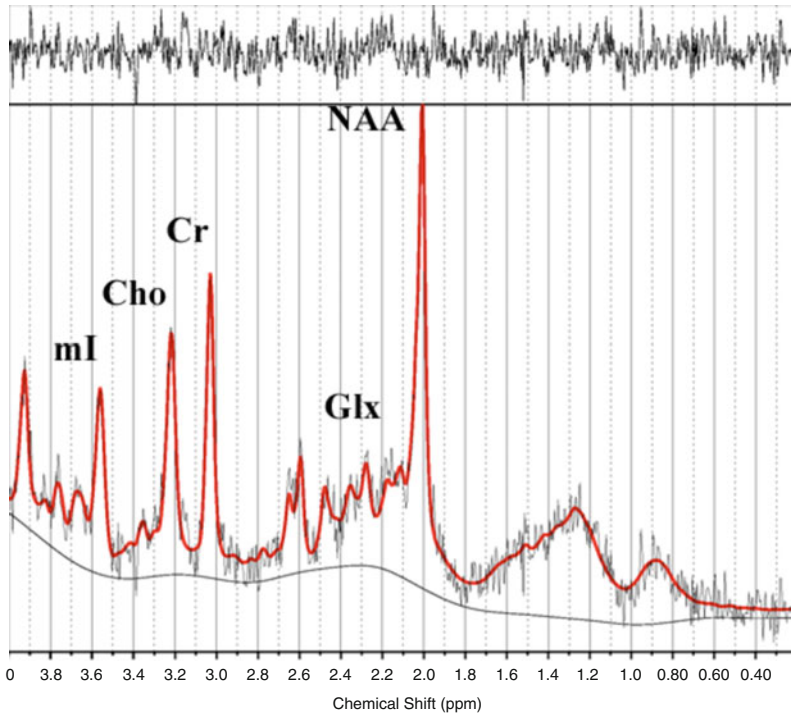

Fig. 28.2 A typical in vivo example of linear combination model spectrum in the same area with metabolite peaks. mI: myo-inositol; Chow: Choline compounds; Cr: creatine, Glx: glutamate + glutamine; NAA: N-acetyl-aspartate

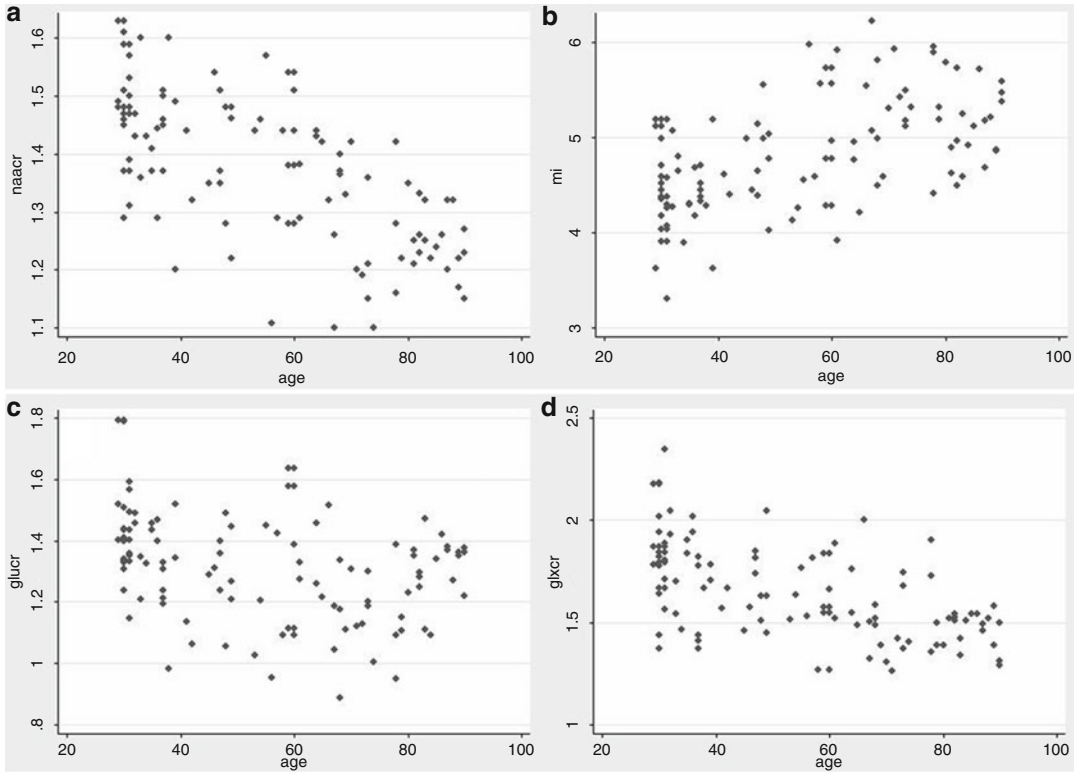

Fig. 28.3 Metabolite levels controlling for age and gender. NAA/Cr (**a**), Glu/Cr (**c**) and Glx/Cr (**d**) ratios show a negative correlation with age, while mI (**b**) show a direct correlation

[15, 16] are also found. Decreased NAA has been documented in patients with AD. This reduction may reflect a combination of the loss of neural cells, reduced neural metabolism, loss of dendritic structures, and reduced myelination. As NAA is almost entirely located within neurons in the central nervous system, the reduced neuronal density may reflect neuronal death or decreased tissue volume. As the reduced NAA signal could be interpreted as a sign of neuronal dysfunction, it does not necessarily indicate cell death. The depletion of NAA concentration could reflect decreased mitochondrial metabolism, which may correlate with the patient's age. There are cross-sectional studies dealing with MRS in AD. A study including 206 normal elderly subjects and 121 patients with AD demonstrated a decrease in the NAA/Cr ratios as well as increased mI/Cr and Chow/Cr ratios in the left posterior cingulate gyrus in patients with AD as compared with controls [17]. Some studies suggest a continuum between normal aging, MCI, and AD with regard to the values of NAA in the brain [18, 19].

Longitudinal studies also confirm the utility of MRS as biomarker. The use of spectroscopy in the occipital cortex and posterior cingulated aiming to determine the rate of NAA/Cr, may be a valid tool for predicting the conversion of MCI to AD. It has been demonstrated that receiver operator curve analysis for NAA/Cr <1.61 predicted conversion with 100 % sensitivity and 75 % specificity [20]. The area under the curve was 0.91 with a positive predictive value of 83 % and a negative predictive value of 100 % with 88.7 % correct classification. Similarly [21], it has been shown that NAA/Cr <1.40 in the posterior cingulate predicted conversion of MCI to probable AD with sensitivity of 82 % and specificity of 72 % and an area under the curve of 0.82 and correlates closely with clinical severity scales [22].

Finally [23], showed that NAA/Cr <1.43 in the posteromedial parietal cortex predicted conversion to probable AD with 74 % sensitivity and 84 % specificity and an area under the curve of 0.84.

Additional longitudinal studies showed valuable results with magnetic resonance spectroscopy. In a large cohort of 151 MCI patients (most of them being of amnestic type) followed-up for 3 years, MRS was individually predictive of conversion to dementia but the accuracy of prediction improved when MRS was used in combination with hippocampal volumetry and the presence of cortical infarctions [24].

The value of proton MRS as a biomarker was assessed ante-mortem in a single study with 54 patients ranging from low to high likelihood of having AD and who underwent autopsy. Decreases in NAA/Cr and increases in myo-inositol/Cr ratios in the posterior bilateral cingulate gyrus correlated with higher postmortem Braak neurofibrillary tangle staging [25]. Godbolt and coworkers [26] noted that presymptomatic ApoE 4 subjects had decreased levels of NAA/myo-inositol and NAA/Cr by 10–25 % compared to controls, and that these differences appeared years before clinical symptoms [26]. Kantarci and his group found that the choline/Cr ratios decreased for 13 months in stable patients with MCI, whereas no changes were seen in patients with MCI progressing to AD. This may reflect a compensatory cholinergic mechanism failing in MCI patients who progress to AD [27].

There is also a growing appreciation of common risk factors for AD and vascular dementias (VaD), and that both pathologies may contribute to cognitive decline in an individual. Other primary degenerative dementias, such as fronto-temporal degeneration (FTD) may present atypically. Consequently there may be considerable overlap between clinical and imaging features in these conditions.

Metabolic changes in fronto-temporal dementia are similar to Alzheimer's disease, with low levels of NAA/Cr and higher than normal levels of myo-inositol/Cr [28]. MRS studies in common dementias are limited to comparing the signs of MRS in Alzheimer's disease with other dementias such as fronto-temporal dementia [29, 30], vascular dementia and Parkinson disease [31].

It is important to note that the reliability of these values requires a good reproducibility and depends more on the technical characteristics of the study of resonance (magnetic field homogeneity, good signal to noise ratio, peak width of the metabolites) than post-processing methods [32].

Monitoring of Treatment

With the recent availability of many pharmaceutical agents modestly effective for treating symptoms of AD, medicine has entered a new era in treating AD. Neuroimaging may provide a useful tool for monitoring the progression of AD. Several published trials measured the effect of drugs on AD progression with MRS and, we can see in general that drugs produced small changes in metabolite levels and ratios which correlated with the modest clinical or no effect of the drugs on AD progression. Decreases in choline/Cr and choline/phosphocreatine in parietal cortex in comparison with controls have been demonstrated using MRS in patients with AD when receiving xanomeline, a muscarinic agonist [33]. Decreased choline/Cr ratios in patients with AD when treated with cholinergic agonists [34] and increased NAA/Cr were detected under treatment with donepezil, a cholinesterase inhibitor [35].

A randomized trial included 67 patients who were treated with either donepezil or placebo for 1 year [36]. The NAA levels elevated transiently in the donepezil group at week 12 and 18 but the differences were not significant at endpoint, and cognitive improvement correlated with NAA elevations in the cortex. Conversely, in the placebo group the NAA concentration tended to remain near baseline values or to decrease modestly [36]. By comparison, other studies have found only a slight increase of NAA/Cr in patients with AD when treated with rivastigmine [37]. In a randomized trial, donepezil and memantine were compared by analysis of metabolite values in several areas of the brain. The general trend was towards a small elevation of NAA/Cr ratios. However, the results were not statistically significant. In the global sample there was a significant correlation between the clinical changes and changes in NAA/Cr values [38]. A recently published study, including 42 patients with AD and 22 controls all of whom underwent six MRS

studies over a 2-year timespan, showed that there is a progressive decline in the NAA/Cr ratios independent of treatment with cholinesterase inhibitors, which is consistent with the lack of efficacy of these drugs [39].

Glutamate is another neurotransmitter studied with MRS. Increased glutamatergic excitotoxicity has been reported in AD but several cross-sectional reports showed decreased levels of glutamate in AD in comparison with controls. In a small open trial, galantamine treatment for 4 months tended to elevate glutamate levels in the hippocampus [40].

Diffusion Tensor Imaging

White Matter Structure

Neuroimaging reveals changes in the white matter (WM) structure in the human brain. WM comprises half of the human brain and consists of bundles of myelinated axons connecting neurons in different brain regions [41]. Grey matter is composed of neuronal cell bodies and dendrites concentrated in the outer layers of the cortex.

Microstructural changes in WM can be revealed by specialized MRI brain imaging techniques such as DTI. This method analyzes the diffusion of protons in tissue, which is more restricted in WM than in grey matter.

DTI Measurement

Water molecules in the brain are in constant Brownian motion, and although the movement of these protons affects conventional structural imaging, diffusion weighted imaging (DWI) and DTI allow quantification of this microscopic movement within each voxel. The main advantage of using diffusion tensor imaging, rather than DWI, is that DTI reflects the underlying diffusion properties of the sample independent of the orientation of the tissue with respect to the direction of measurements (See Fig. 28.4). DTI is thus a robust quantitative technique that is independent of how the subject has been oriented inside the scanner magnet and gradient coils. In regions with few or no constraints imposed by physical boundaries, such as cerebrospinal fluid (CSF) in the ventricles, water movement is random in every direction and is isotropic. In contrast to CSF, the path of a water molecule in a

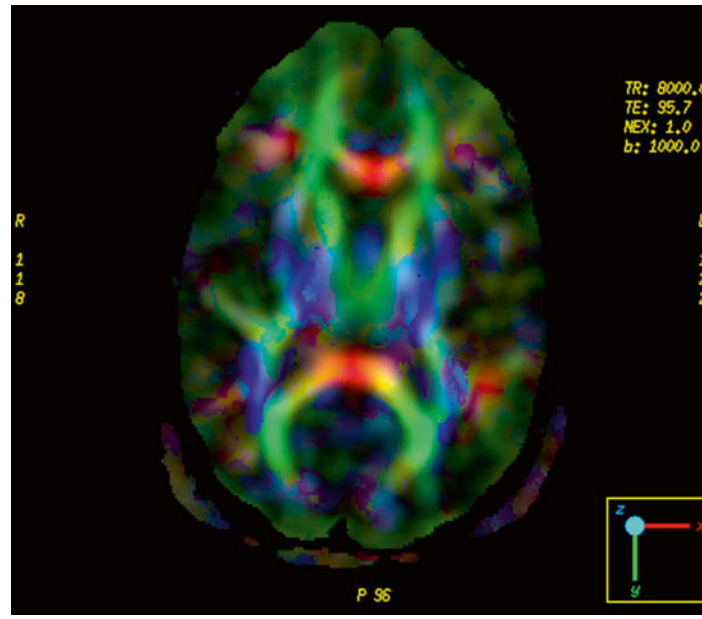

Fig. 28.4 Diffusion tensor imaging and example of color-encoded fiber orientation maps. Fibers that are predominantly oriented *left–right* are shown in *red*, anterior–posterior fibers are shown in *green*, and superior–inferior fibers are shown in *blue*

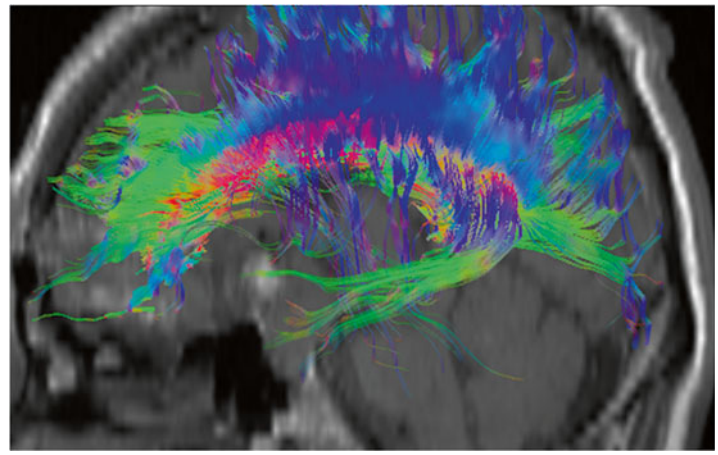

Fig. 28.5 3D DTI-based reconstruction results of association fibers in the limbic system (*green*) and corpus callosum (*blue*)

WM fiber is constrained by physical boundaries such as the axon sheath, causing the movement along the long axis of a fiber to be greater than across the radial diffusion. These data can be used to calculate the probable anatomy of WM bundles in living brain, a process called tractography (See Fig. 28.5). Orientation is calculated from the eigenvectors defining proton diffusion in three dimensions in each voxel. Using algorithms, the principal eigenvalue vector is connected to the next voxel to trace the fiber structure and orientation in WM tracts.

DTI yields quantitative measures for tissue water mobility as a function of the direction of water motion and is probed by application of diffusion sensitization gradients in multiple directions. Baser and coworkers [42] described the use of multivariate linear regression to calculate diffusivity, D, from a non-diffusion-weighted image plus six or more diffusion-weighted measurements in a non-collinear direction. The diffusion weighting is obtained by simultaneously applying diffusion gradients along combinations of the three physical axes.

The appropriate mathematical combination of the directional diffusion-weighted images provides quantitative measures of water diffusion for each voxel via the apparent diffusion coefficient (ADC), as well as the degree of diffusion directionality, or anisotropy. The anisotropy increases with increased myelination, diameter, and axon compaction. Myelin is a major diffusion barrier for water, and gives WM its high anisotropy. Demyelinating diseases are characterized by partial or total loss of myelin, with consequent loss of neuronal function.

MCI and AD

Increase in the ADC has been described in multiple regions of WM, corpus callosum, and cingulum of patients with AD as compared with controls [43]. Huang and coworkers [44] found functionally relevant microstructural changes in patients with AD and MCI. These changes were present in brain regions with high cortical functions, but not in regions of primary functions, and are consistent with a hypothetical decrease in axonal process in the temporal lobe [44].

Neuroimaging in MCI and AD generally shows medial temporal lobe atrophy and diminished glucose metabolism in the posterior cingulate gyrus. However, it is unclear whether these abnormalities also impact the cingulum fibers, which connect the medial temporal lobe and the posterior cingulate regions. Assessment of the cingulum fibers using DTI may be of help for an early diagnosis of AD [45].

It was proposed in a recent review that using analysis of regional mean fractional anisotropy (FA) and mean diffusivity (MD) values, it was possible to show that MD values are different in all WM regions of the brain between controls and AD patients, and that FA showed similar results except for the parietal lobe and internal capsule [46]. Furthermore, a few studies in healthy older subjects at risk for AD showed abnormalities in

MD values in regions known to be affected in AD [47, 48]. Besides showing early alterations in MCI patients, DTI appears to correlate with cognitive performance independent of cortical atrophy, which suggests access to an upstream process in the neurodegenerative cascade [49]. The search for appropriate DTI and high angular resolution diffusion imaging parameters for the diagnosis of cognitive impairment is still a work in progress [50]. Various parameters behave in different ways according to localization [51]. In addition to the choice of diffusion parameters, recent tractography studies illustrate the superiority of analysis methods that can manage crossing fibers [52].

Perfusion MRI

PET and single-photon emission computed tomography (SPECT) have been used to identify focal changes in regional cerebral blood flow in patients with MCI and AD. However, the low spatial resolution of PET and SPECT, and the ionizing radiation emitted from the nuclear medicine tracers are major concerns. PET imaging offers a variety of techniques that have a significant role in investigating patients with cognitive impairment. Amyloid imaging with [11C]-labeled Pittsburgh compound-B (PIB) amyloid and [18 F]flurodeoxy glucose PET are covered elsewhere. A molecular probe with high affinity to tubulin associated unit fibrils and a low affinity for synthetic amyloid-β1–42 fibrils is in the early phase of development [53].

Magnetic resonance perfusion techniques have also been developed and offer higher spatial resolution without the use of ionizing radiation [54]. Magnetic resonance perfusion techniques are based on exogenous or endogenous tracers. In the method based on exogenous tracers, a paramagnetic agent such as gadolinium dimeglumine gadopentate is injected, and the resulting decrease and subsequent recovery of the magnetic resonance signal is used to estimate perfusion (See Fig. 28.6). In the method using endogenous tracers, the magnetization of the spins of arterial water are noninvasively labeled using radiofrequency pulses, and the regional accumulation of the label is measured in the tissues by comparison with an image acquired without labeling. In the case of ASL, there is no need to use exogenous contrast material; it uses endogenous water magnetization as diffusible tracer and works with modifications of the magnetization state of blood [55]. Arterial spin labeling-MRI studies of patients with AD and MCI have reported a similar pattern of regional hypoperfusion to that described in previous PET and SPECT studies. Moreover, arterial spin labeling-MRI offers several advantages over PET and SPECT: (1) it is free of exposure to ionizing radiation, intravenous contrast agents, and radioactive isotopes; and (2) it can be rapidly repeated because labeled water is cleared after a few seconds. An additional advantage is that perfusion and structural images can be acquired at the same imaging session.

Previous studies using this method have shown hypoperfusion in some brain areas in patients with MCI and AD compared with controls, including the right inferior parietal, bilateral posterior cingulate gyri, and bilateral middle frontal gyri, a pattern of hypoperfusion that is similar to the one seen with PET and SPECT scan studies in this population [56, 57]. Chao and coworkers [58] compared the predictive value of cerebral perfusion as measured by arterial spin labeling-MRI with magnetic MRI hippocampal volume for determining future cognitive and functional decline and subsequent conversion from MCI to dementia [58]. Results from linear mixed effects modeling suggest that baseline perfusion from the right precuneus predicted subsequent declines in the Clinical Dementia Rating, Functional Activities Questionnaire, and selective attention, whereas baseline hypoperfusion in the right middle frontal cortex predicted subsequent episodic memory decline in the California Verbal Learning Test. These results suggest that hypoperfusion as detected by arterial spin labeling-MRI can predict subsequent clinical, functional, and cognitive decline and may be useful in identifying candidates for future AD treatment trials.

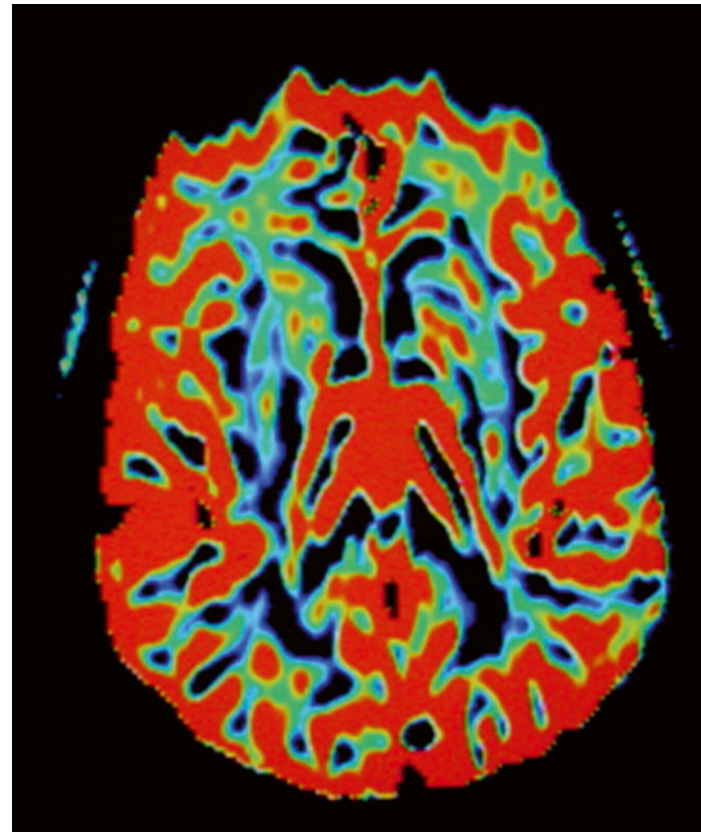

Fig. 28.6 Example of cerebral perfusion contrast-enhanced dynamic susceptibility. (DSC) with decreased left frontal cerebral blood

Structural Neuroimaging

Structural neuroimaging has also been validated as a tool in the detection and progression monitoring of preclinical AD. In AD there is cortical atrophy including thinning of gyri, widening of sulci, thinning of the cortical ribbon (coronal plane), reduced volume of the centrum semiovale, and lateral ventricular enlargement (one third of cases). The atrophy is evident in the medial temporal lobe, particularly the amygdala, hippocampus, and parahippocampal gyrus. Temporal lobe MRI may have an important role in assisting with the clinical diagnosis of AD, particularly its differentiation from other disorders that may cause diagnostic difficulties in the clinical practice. Tissue volumes in the central nervous system, and in particular changes in volume over time, are sensitive markers of a range of neurological disease states and disease progression. Measurement of brain volume requires segmentation of the brain from the rest of the tissues in the head and neck. While this can be performed manually or in a semiautomated manner, automated procedures are likely to be more reproducible and rapid. This is understandable because the size of the structures involved is usually relatively small, making the analysis less tedious than a manual segmentation of the whole brain. Manual segmentation to measure the hippocampal volume is recognized as the gold standard. However, an initial survey of the 12 most cited manual segmentation protocols revealed a 2.5-fold volume measurement difference [59]. The group that included Barnes performed a meta-analysis of hippocampal atrophy rates in patients with AD and matched controls from studies reported in the peer-reviewed literature [60]. Meta-analysis and meta-regression were then

performed with nine studies from seven centers, a total of 595 patients with AD and 212 matched controls. They found strong evidence of between-study heterogeneity, and finally concluded that the overall hippocampal atrophy rate was 1.4 % in normal controls with an age range of between 69 and 83 years. In patients with AD, the overall atrophy rate was 4.6 %. Automated validated measures of hippocampal volume will help to increase reproducibility of results. Additionally, many structures such as the hippocampus, are difficult to segment in an automated manner, but are relatively easily identified and manually or semiautomatically outlined, given the appropriate software. Some progress has been made in automating segmentation procedures, with methods including the use of deformable shape models.

Tensor-based morphometry (TBM) is a relatively new image analysis technique that identifies regional structural differences in the brain, across groups, or over time from the gradients of the deformation fields that warp images to a common anatomical template. The anatomical information is encoded in the spatial transformation (See Fig. 28.7). Therefore, accurate inter-subject non-rigid registration is an essential tool. With the advent of recent and powerful non-rigid registration algorithms based on the large deformation paradigm, TBM is being increasingly used [61] but at the moment is restricted mostly to research settings. Various automated methods to classify people with AD and MCI using structural MRI T1- weighted images have been proposed and have been reviewed [62]. The authors concluded that most of the techniques accurately classified normal controls and patients with AD. However, these methods had lower sensitivity in diagnosing prodromal AD. Again, the diagnostic value of specific hippocampal atrophy measurements has been well established in referral clinic populations, but its diagnostic value has not been demonstrated in unselected primary care patients, and this will remain a challenge for the foreseeable future.

fMRI

Another more recent imaging method for the mapping of activation patterns in the brain is fMRI. This is an important technique for better understanding brain function. When a brain region is activated, new energy must be transported to this region which leads to increased blood flow to that part of the brain. This can be

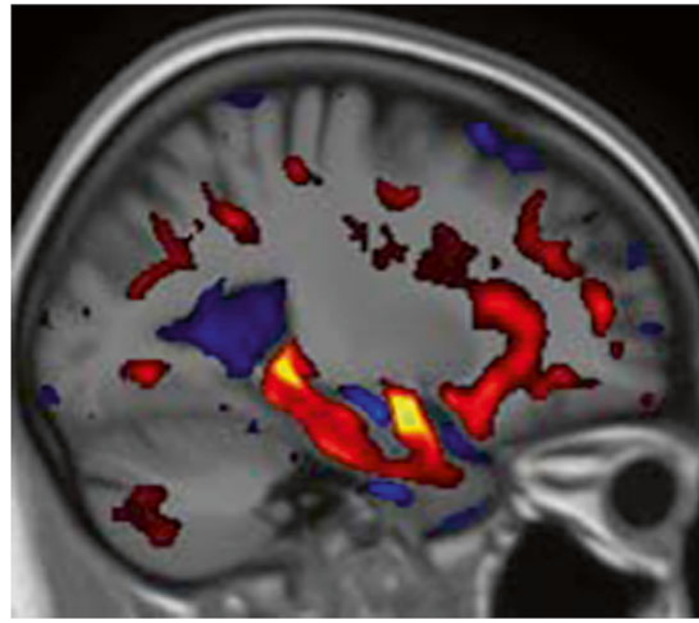

Fig. 28.7 Example tensor based morphometry of the AD patients vs. controls subjects. Statistical significance maps show dilatation (*blue*) and contraction brain volume (*yellow* and *red*) in AD

imaged by repetitive magnetic resonance scans and detected by appropriate signal processing methods.

Episodic memory encoding function is most commonly investigated because of its early and consistent involvement in AD. During episodic memory encoding, patients with AD onsistently show lower activation in medial temporal lobe structures, particularly the hippocampus [63], failure of the normal deactivation in posteromedial cortical areas such as the posterior cingulate and medial parietal cortex, [64] and increased activation in the prefrontal cortex, probably as a compensation mechanism [65]. fMRI studies have shown a decrease in intensity and/or extent of activation in the frontal and temporal region of patients with AD compared with normal subjects. In the genetic risk groups (ApoE4), activation with memory tasks has been shown greater extent and intensity of frontal and temporal brain activation, suggesting a compensatory brain function [35].

Dickerson and coworkers have extended a preliminary analysis of functional magnetic MRI as a predictor of dementia in MCI. Over a follow-up interval of more than 5 years after functional MRI scanning in 25 MCI subjects, some did not show change and others progressed to dementia [66]. The degree of cognitive decline was predicted by hippocampal activation at the time of baseline scanning, with greater hippocampal activation predicting greater decline. These data suggest that functional MRI may provide a physiologic imaging biomarker useful for identifying the subgroup of MCI individuals at highest risk of cognitive decline for potential inclusion in disease-modifying clinical trials.

The brain network referred to as the default mode network (DMN) includes several cortical areas that are particularly active at rest and deactivate during cognitive tasks. This network includes the medial prefrontal cortex, posterior cingulate cortex, precuneus, anterior cingulate cortex, and parietal cortex. The hippocampus is functionally connected to this network. A significant alteration in the intrinsic functional connectivity between the hippocampus and areas in the DMN at rest and during cognitive tasks in patients with MCI and AD has been reported [67].

Summary, Conclusions, and Future Directions

Several techniques used for the diagnosis of MCI and AD have been discussed in this chapter. Structural MRI alone has also proven insufficient to predict early AD and additional biomarkers are needed in combination to make reliable predictions in MCI. Additionally, an excess of significance bias has been suggested in volumetric studies according to data synthesis from 41 meta-analysis [68]. At present, there are no other non-invasive techniques that can provide equivalent information and, as a consequence, MRI, DTI tractography, and fMRI are expected to be a powerful combined technique for researching brain anatomy and disease in situ in human beings [69]. MRS in combination with DTI and fMRI may provide clinicians with information about ongoing pathological changes in AD. DTI and MRI are non-invasive and do not require the use of radioactive tracers, suggesting its potential safe application for longitudinal follow-up and repeated assessments. Mandal and coworkers have shown that brain oxidative stress can be determined non-invasively and quantified in various regions of the brain in both healthy young male and female subjects as well as in patients with MCI and AD [70]. It was also demonstrated using MRS technique that detection of glutathione in specific brain region may provide crucial information related to clinical status. In order to have diagnostic value in the individual patient with these neuroimaging modalities, they must have established validity, sensitivity, specificity, predictive value, and test–retest and interrater reliability.

The MRI scans show that the death of brain cells precedes symptoms of AD by 5 or 6 years. The goal of newer imaging methods is to detect these changes even earlier, and more precisely track disease progression. The accumulation of neurodegenerative biomarker abnormalities might reflect a more severe brain pathological stage that could potentially increase the risk of longitudinal cognitive decline [71] as well as development of clinical AD [72–74].

A recent study comparing neuroimaging modalities for the prediction of conversion from

mild cognitive impairment to Alzheimer dementia shows that among individual modalities, MRI had the highest predictive accuracy (67 %), which increased from 9 % to 76 % when combined with PIB-PET, producing the highest accuracy among any biomarker combination. Individually, PIB-PET generated the best sensitivity, and fluorodeoxyglucose PET had the lowest. Among individual brain regions, the temporal cortex was found to be most predictive for MRI and PIB-PET [75].

Larger longitudinal studies with improved homogeneity of participants and methods, combining neuroimaging and other diagnostic data, will probably give to the modalities discussed in this chapter clinical utility in the near future. The improvements in brain imaging techniques will help scientists working with AD to better understand this devastating and deadly cognitive decline.

References

1. Petersen RC, Smith GE, Waring SC, Ivnik RJ, Tangalos EG, Kokmen E. Mild cognitive impairment. Clinical characterization and outcome. Arch Neurol. 1999;56:303–8.
2. Turner RS. Biomarkers of Alzheimer's disease and mild cognitive impairment: are we there yet? Exp Neurol. 2003;183:7–10.
3. Savva GM, Wharton SB, Ince PG, Ince PG, Forster G, Matthews FE, Brayne C. Age, neuropathology, and dementia. N Engl J Med. 2009;360:2302–9.
4. Sitoh YY, Kanagasabai K, Earnest A, Sahadevan S. Evaluation of dementia: the case for neuroimaging all mild to moderate cases. Ann Acad Med Singapore. 2006;35:383–9.
5. Sauter R, Schneider K, Wicklow K, Kolem H. Localized1H MRS of the human brain: single voxel versus CSI techniques. J Magn Reson Imaging. 1991;1:241.
6. Hsu YY, Chen MC, Lim KE, Chang C. Reproducibility of hippocampal single-voxel proton MR spectroscopy and chemical shift imaging. Am J Roentgenol. 2001; 176:529–36.
7. Maheshwari SR, Fatterpekar GM, Castillo M, Mukherji SK. Proton MR spectroscopy of the brain. Semin Ultrasound CT MR. 2000;21:434–51.
8. Fayed N, Olmos S, Morales H, Modrego PJ. Physical basis of magnetic resonance spectroscopy and its application to central nervous system diseases. Am J Appl Sci. 2006;3:1836–45.
9. Hancu I, Zimmerman EA, Sailasuta N, Hurd RE. 1H MR spectroscopy using TE averaged PRESS: a more sensitive technique to detect neurodegeneration associated with Alzheimer's disease. Magn Reson Med. 2005;53:777–82.
10. Provencher SW. Estimation of metabolite concentrations from localized in vivo proton NMR spectra. Magn Reson Med. 1993;30:672–9.
11. Rapoport SI. Hydroge n magnetic resonance spectroscopy in Alzheimer's disease. Lancet Neurol. 2002;1:82.
12. Modrego PJ. Predictors of conversion to dementia of probable Alzheimer type in patients with mild cognitive impairment. Curr Alzheimer Res. 2006;3:161–70.
13. Valenzuela MJ, Sachdev P. Magnetic resonance spectroscopy in AD. Neurology. 2001;56:592–8.
14. Siger M, Schuff N, Zhu X, Miller BL, Weiner MW. Regional myo-inositol concentration in mild cognitive impairment using 1H magnetic resonance spectroscopic imaging. Alzheimer Dis Assoc Disord. 2009;23:57–62.
15. Rupsingh R, Borrie M, Smith M, Wells JL, Bartha R. Reduced hippocampal glutamate in Alzheimer disease. Neurobiol Aging. 2011;32:802–10.
16. Fayed N, Modrego PJ, Rojas-Salinas G, Aguilar K. Brain glutamate levels are decreased in Alzheimer's disease: a magnetic resonance spectroscopy study. Am J Alzheimers Dis Other Demen. 2011;26:450–6.
17. Kantarci K, Petersen RC, Boeve BF, Knopman DS, Tang-Wai DF, O'Brien PC, Weigand SD, Edland SD, Smith GE, Ivnik RJ, Ferman TJ, Tangalos EG, Jack Jr CR. 1H MR spectroscopy in common dementias. Neurology. 2004;63:1393–8.
18. Parnetti L, Lowenthal DT, Presciutti O, Pelliccioli GP, Palumbo R, Gobbi G, Chiarini P, Palumbo B, Tarducci R, Senin U. 1 H-MRS, MRI-based hippocampal volumetry, and 99mTc-HMPAO-SPECT in normal aging, age-associated memory impairment, and probable Alzheimer's disease. J Am Geriatr Soc. 1996;44:133–8.
19. Kantarci K, Xu Y, Shiung MM, O'Brien PC, Cha RH, Smith GE. Comparative diagnostic utility of different MR modalities in mild cognitive impairment and Alzheimer's disease. Dement Geriatr Cogn Disord. 2002;14:198–207.
20. Modrego PJ, Fayed N, Pina MA. Conversion from mild cognitive impairment to probable Alzheimer's disease predicted by brain magnetic resonance spectroscopy. Am J Psychiatry. 2005;162:667–75.
21. Fayed N, Davila J, Oliveros A, Castillo J, Medrano JJ. Utility of different MR modalities in mild cognitive impairment and its use as a predictor of conversion to probable dementia. Acad Radiol. 2008;15:1089–98.
22. Fayed N, Dávila J, Oliveros A, Medrano J, Castillo J. Correlation of findings in advanced MR techniques with global severity scales in patients with some grade of cognitive impairment. Neurol Res. 2010;32:157–65.
23. Modrego PJ, Fayed N, Sarasa M. Magnetic resonance spectroscopy in the prediction of early conversion from amnestic mild cognitive impairment to dementia: a prospective cohort study. BMJ Open. 2011;1:e000007.
24. Kantarci K, Weigand SD, Przybelski SA, Shiung MM, Whitwell JL, Negash S, Knopman DS, Boeve

BF, O'Brien PC, Petersen RC, Jack Jr CR. Risk of dementia in MCI. Combined effect of cerebrovascular disease, volumetric MRI, and H MRS. Neurology. 2009;72:1519–25.
25. Kantarci K, Knopman DS, Dickson DW, Parisi JE, Whitwell JL, Weigand SD, Josephs KA, Boeve BF, Petersen RC, Jack Jr CR. Alzheimer disease: postmortem neuropathologic correlates of antemortem 1-H MR Spectroscopy metabolite measurements. Radiology. 2008;248:210–20.
26. Godbolt AK, Waldman AD, MacManus DG, Schott JM, Frost C, Cipolotti L. MRS shows abnormalities before symptoms in familial Alzheimer disease. Neurology. 2006;66:718–22.
27. Kantarci K, Weigand SD, Petersen RC, Boeve BF, Knopman DS, Gunter J. Longitudinal 1H MRS changes in mild cognitive impairment and Alzheimer's disease. Neurobiol Aging. 2007;28:1330–9.
28. Ernst T, Chang L, Melchor R, Mehringer CM. Frontotemporal dementia and early Alzheimer disease: differentiation with frontal lobe H-1 MR spectroscopy. Radiology. 1997;203:829–36.
29. MacKay S, Ezekiel F, Di Sclafani V, Meyerhoff DJ, Gerson J, Norman D. Alzheimer disease and subcortical ischemic vascular dementia: evaluation by combining MR imaging segmentation and H-1 MR spectroscopic imaging. Radiology. 1996;198:537–45.
30. MacKay S, Meyerhoff DJ, Constans JM, Norman D, Fein G, Weiner MW. Regional gray and white matter metabolite differences in subjects with AD, with subcortical ischemic vascular dementia, and elderly controls with 1H magnetic resonance spectroscopic imaging. Arch Neurol. 1996;53:167–74.
31. Firbank MJ, Harrison RM, O'Brien JT. A comprehensive review of proton magnetic resonance spectroscopy studies in dementia and Parkinson's disease. Dement Geriatr Cogn Disord. 2002;14:64–76.
32. Fayed N, Modrego PJ, Medrano J. Comparative test-retest reliability of metabolite values assessed with magnetic resonance spectroscopy of the brain. The LCModel versus the manufacturer software. Neurol Res. 2009;31:472–7.
33. Satlin A, Bodick N, Offen WW, Renshaw PF. Brain proton magnetic resonance spectroscopy (1H-MRS) in Alzheimer's disease: changes after treatment with xanomeline, an M1 selective cholinergic agonist. Am J Psychiatry. 1997;154:1459–61.
34. Frederick B, Satlin A, Wald LL, Hennen J, Bodick N, Renshaw PF. Brain proton magnetic resonance spectroscopy in Alzheimer disease: changes after treatment with xanomeline. Am J Geriatr Psychiatry. 2002;10:81–8.
35. Petrella JR, Coleman RE, Doraiswamy PM. Neuroimaging and early diagnosis of Alzheimer disease: a look to the future. Radiology. 2003;226: 315–36.
36. Krishnan KR, Charles HC, Doraiswamy PM, Mintzer J, Weisler R, Yu X, Perdomo C, Ieni JR, Rogers S. Randomized, placebo-controlled trial of the effects of donepezil on neuronal markers and hippocampal volumes in Alzheimer disease. Am J Psychiatry. 2003;160:2003–11.
37. Modrego PJ, Pina MA, Fayed N, Díaz M. Changes in metabolite ratios after treatment with rivastigmine in Alzheimer's disease: a nonrandomised controlled trial with magnetic resonance spectroscopy. CNS Drugs. 2006;20:867–87.
38. Modrego PJ, Fayed N, Errea JM, Rios C, Pina MA, Sarasa M. Memantine versus donepezil in mild to moderate Alzheimer's disease: a randomized trial with magnetic resonance spectroscopy. Eur J Neurol. 2010;17:405–12.
39. Schott JM, Frost C, Macmanus DG, Ibrahim F, Waldman AD, Fox ND. Short echo time proton magnetic resonance spectroscopy in Alzheimer's disease: a longitudinal multiple time point study. Brain. 2010;133:3315–22.
40. Penner J, Rupsingh R, Smith M, Wells JL, Borrie MJ, Bartha R. Increased glutamate in the hippocampus after galantamine treatment for Alzheimer disease. Prog Neuropsychopharmacol Biol Psychiatry. 2010; 34:104–10.
41. Fields RD. White matter in learning, cognition and psychiatric disorders. Trends Neurosci. 2008;31: 317–76.
42. Basser PJ, Pierpaoli C. Microstructural and physiological features of tissues elucidated by quantitative-diffusion-tensor MRI. J Magn Reson B. 1996; 111:209–19.
43. Ramani A, Jensen JH, Helpern JA. Quantitative MR imaging in Alzheimer disease. Radiology. 2006;241: 26–44.
44. Huang J, Friedland RP, Auchus AP. Diffusion tensor imaging of normal-appearing white matter in mild cognitive impairment and early Alzheimer disease: preliminary evidence of axonal degeneration in the temporal lobe. AJNR Am J Neuroradiol. 2007;28: 1943–8.
45. Zhang Y, Schuff N, Jahng G, Bayne W, Mori S, Schad L, Mueller S, Du T, Kramer J, Yaffe K, Chui H, Jagust W, Miller B, Weiner M. Diffusion tensor imaging of cingulum fibers in mild cognitive impairment and Alzheimer disease. Neurology. 2007;68:13–9.
46. Sexton CE, Kalu UG, Filippini N, Mackay CE, Ebmeier KP. A meta-analysis of diffusion tensor imaging in mild cognitive impairment and Alzheimer's disease. Neurobiol Aging. 2011;32:2322.
47. Bendlin BB, Ries ML, Canu E, Sodhi A, Lazar M, Alexander AL, Carlsson CM, Sager MA, Asthana S, Johnson SC. White matter is altered with parental family history of Alzheimer's disease. Alzheimers Dement. 2010;6:394–403.
48. Gold BT, Johnson NF, Powell DK, Smith CD. White matter integrity and vulnerability to Alzheimer's disease: preliminary findings and future directions. Biochim Biophys Act. 1822;2012:416–22.
49. Grambaite R, Reinvang I, Selnes P, Fjell AM, Walhovd KB, Stenset V, Fladby T. Pre-dementia memory

impairment is associated with white matter tract affection. J Int Neuropsychol Soc. 2011;17:143–53.
50. Bozoki AC, Korolev IO, Davis NC, Hoisington LA, Berger KL. Disruption of limbic white matter pathways in mild cognitive impairment and Alzheimer's disease: a DTI/FDG-PET study. Hum Brain Mapp. 2012;33:1792–802.
51. Wang PN, Chou KH, Lirng JF, Lin KN, Chen WT, Lin CP. Multiple diffusivities define white matter degeneration in amnestic mild cognitive impairment and Alzheimer's disease. J Alzheimers Dis. 2012;30:423–37.
52. Douaud G, Jbabdi S, Behrens TE, Menke RA, Gass A, Monsch AU, Rao A, Whitcher B, Kindlmann G, Matthews PM, Smith S. DTI measures in crossing-fibre areas: increased diffusion anisotropy reveals early white matter alteration in MCI and mild Alzheimer's disease. Neuroimage. 2011;55:880–90.
53. Fodero-Tavoletti MT, Okamura N, Furumoto S, Mulligan RS, Connor AR, McLean CA, Cao D, Rigopoulos A, Cartwright GA, O'Keefe G, Gong S, Adlard PA, Barnham KJ, Rowe CC, Masters CL, Kudo Y, Cappai R, Yanai K, Villemagne VL. 18F-THK523: a novel in vivo tau imaging ligand for Alzheimer's disease. Brain. 2011;134(Pt 4):1089–100.
54. Belliveau JW, Rosen BR, Kantor HL, Rzedzian RR, Kennedy DN, McKinstry RC, Vevea JM, Cohen MS, Pykett IL, Brady TJ. Functional cerebral imaging by susceptibility-contrast NMR. Magn Reson Med. 1990;14:538–46.
55. Fayed-Miguel N, Castillo-Blandino J, Medrano-Lin J. Perfusion by magnetic resonance imaging: its physical foundations and clinical application. Rev Neurol. 2010;50:23–32.
56. Johnson NA, Jahng GH, Weiner MW, Miller BL, Chui HC, Jagust WJ, Gorno-Tempini ML, Schuff N. Pattern of cerebral hypoperfusion in Alzheimer disease and mild cognitive impairment measured with arterial spin labeling MR imaging: initial experience. Radiology. 2005;234:851–9.
57. Alsop DC, Detre JA, Grossman M. Assessment of cerebral blood flow in Alzheimer's disease by spin-labeled magnetic resonance imaging. Ann Neurol. 2000;47:93–100.
58. Chao LL, Shannon W, Buckley ST, Kornak J, Schuff N, Madison C, Yaffe K, Miller B, Kramer J, Weiner M. ASL perfusion MRI predicts cognitive decline and conversion from MCI to dementia. Alzheimer Dis Assoc Disord. 2010;24:19–27.
59. Boccardi M, Ganzola R, Bocchetta M, Pievani M, Redolfi A, Bartzokis G, Camicioli R, Csernansky JG, de Leon MJ, de Toledo-Morrell L, Killiany RJ, Lehéricy S, Pantel J, Pruessner JC, Soininen H, Watson C, Duchesne S, Jack Jr CR, Frisoni GB. Survey of protocols for the manual segmentation of the hippocampus: preparatory steps towards a joint EADC-ADNI Harmonized Protocol. J Alzheimers Dis. 2011;26:61–75.
60. Barnes J, Bartlett J, Van de Pol L, Loy C, Scahill R, Frost C, Thompson P, Fox NC. A meta-analysis of hippocampal atrophy rates in Alzheimer's disease. Neurobiol Aging. 2009;30:1711–23.
61. Lepore N, Brun C, Chou YY, Chiang MC, Dutton R, Hayashi K, Luders E, Lopez O, Aizenstein H, Toga A, Becker J, Thompson P. Generalized tensor-based morphometry of HIV/AIDS using multivariate statistics on deformation tensors. IEEE Trans Med Imaging. 2008;27:129–41.
62. Li X, Coyle D, Maguire L, Watson DR, McGinnity TM. Gray matter concentration and effective connectivity changes in Alzheimer's disease: a longitudinal structural MRI study. Neuroradiology. 2011;53:733–48.
63. Golby A, Silverberg G, Race E, Gabrieli S, O'Shea J, Knierim K, Stebbins G, Gabrieli J. Memory encoding in Alzheimer's disease: an fMRI study of explicit and implicit memory. Brain. 2005;128:773–87.
64. Miettinen PS, Pihlajamäki M, Jauhiainen AM, Niskanen E, Hänninen T, Vanninen R, Soininen H. Structure and function of medial temporal and posteromedial cortices in early Alzheimer's disease. Eur J Neurosci. 2011;34:320–30.
65. Solé-Padullés C, Bartrés-Faz D, Junqué C, Vendrell P, Rami L, Clemente IC, Bosch B, Villar A, Bargalló N, Jurado MA, Barrios M, Molinuevo JL. Brain structure and function related to cognitive reserve variables in normal aging, mild cognitive impairment and Alzheimer's disease. Neurobiol Aging. 2009;30:1114–24.
66. Dickerson BC, Salat DH, Bates JF, Atiya M, Killiany RJ, Greve DN. Medial temporal lobe function and structure in mild cognitive impairment. Ann Neurol. 2004;56:27–35.
67. Wang Z, Yan C, Zhao C, Qi Z, Zhou W, Lu J, He Y, Li K. Spatial patterns of intrinsic brain activity in mild cognitive impairment and Alzheimer's disease: a resting-state functional MRI study. Hum Brain Mapp. 2011;32:1720–40.
68. Ioannidis JP. Excess significance bias in the literature on brain volume abnormalities. Arch Gen Psychiatry. 2011;68:773–80.
69. Fayed N, Modrego PJ, Salinas GR, Gazulla J. Magnetic resonance imaging based clinical research in Alzheimer's disease. J Alzheimers Dis. 2012;31 Suppl 3:S5–18.
70. Mandal PK, Tripathi M, Sugunan S. Brain oxidative stress: detection and mapping of anti-oxidant marker 'Glutathione' in different brain regions of healthy male/female, MCI and Alzheimer patients using non-invasive magnetic resonance spectroscopy. Biochem Biophys Res Commun. 2012;417:43–8.
71. Jagust W, Gitcho A, Sun F, Kuczynski B, Mungas D, Haan M. Brain imaging evidence of preclinical Alzheimer's disease in normal aging. Ann Neurol. 2006;59:673–81.
72. Dickerson BC, Stoub TR, Shah RC, Sperling RA, Killiany RJ, Albert MS, Hyman BT, Blacker D,

Detoledo-Morrell L. Alzheimer-signature MRI biomarker predicts AD dementia in cognitively normal adults. Neurology. 2011;76:1395–402.
73. den Heijer T, Geerlings MI, Hoebeek FE, Hofman A, Koudstaal PJ, Breteler MMB. Use of hippocampal and amygdalar volumes on magnetic resonance imaging to predict dementia in cognitively intact elderly people. Arch Gen Psychiatry. 2006;63:57–62.
74. Wirth M, Villeneuve S, Haase CM, Madison CM, Oh H, Landau SM, Rabinovici GD, Jagust WJ. Associations between Alzheimer disease biomarkers, neurodegeneration, and cognition in cognitively normal older people. JAMA Neurol. 2013. doi:10.1001/jamaneurol.2013.4013.
75. Trzepacz PT, Yu P, Sun J, Schuh K, Case M, Witte MM, Hochstetler H, Hake A. Alzheimer's disease neuroimaging initiative. Comparison of neuroimaging modalities for the prediction of conversion from mild cognitive impairment to Alzheimer's dementia. Neurobiol Aging. 2002;35:143–51.